#### **Research Article**

Erdener Pehlivan, Gamze Fahriye Pehlivan\*, Ali Alkan

# An Analogical and Analytical Approach to the Burçevi Monumental Tomb

https://doi.org/10.1515/opar-2025-0060 received May 3, 2025; accepted July 20, 2025

**Abstract:** Ancient Anatolia is well known for housing significant artifacts from the Roman period. One such artifact, the Burçevi Monumental Tomb, stands out as a unique example in this region of Anatolia, with no other known parallels, and has not yet been documented in the scientific literature. This study aims to examine the Burçevi Monumental Tomb through both analogical and analytical approaches. The primary goal is to introduce the monument to the archaeological community. In addition to the commonly used analogical methods of archaeology and architectural history, the study integrates innovative analytical techniques. These methods provide insights into the tomb's architecture, chronology, material composition, and structural durability. The results indicate that the Burçevi Monumental Tomb was locally produced. The fact that this structure is the only known example from the second century AD within the borders of Sivas Province underscores its importance as a reflection of Roman Imperial Period burial traditions in Anatolia.

Keywords: monumental tomb, XRF, SHR, cultural heritage

#### 1 Introduction

The tomb examined in this study is located in Burçevi village, 2.5 km west of the Gürün district center, which is at 135 km south of the Sivas<sup>1</sup> city center (Figure 1). To its west lies Kaisareia (Kayseri), and to its east, Melitene (Malatya). The monumental tomb is situated atop a high hill, approximately 1 km south of the village center. The elevation difference between the hill where the tomb is positioned and the Şuğul Valley, where the village is established, has been determined to be 236 m.

The tomb in question likely falls within the territorial boundaries of the ancient settlement of Gauraina, whose precise location within the Roman province of Cappadocia has yet to be determined. The structure appears to offer clues about this settlement. However, the mosaic found in Tepecik village, located 23 km southeast of the Gürün district center, raises questions regarding the localization of Gauraina within a scientific framework. Gauraina was also known as Sargaurasene and is recognized as one of the colony cities in the Cappadocia region (Hild & Restle, 1981, p. 182). This settlement was located along an ancient road route, documented in written sources, that connected Sebasteia (Sivas) and Cucusus (modern Göksun, Kahramanmaraş) (Hild & Restle, 1981, pp. 181–182).

**Erdener Pehlivan:** Department of Archaeology, Sivas Cumhuriyet University, Sivas, Turkey, e-mail: erdener\_pehlivan@hotmail.com **Ali Alkan:** Republic of Türkiye Ministry of Culture and Tourism, Sivas, Turkey, e-mail: ali.alkan@ktb.gov.tr

<sup>1</sup> Although the Sivas city center has been proposed as the location of Sebesteia, the ancient name of Sivas, this hypothesis has not yet been confirmed by archaeological findings. Therefore, the name Sivas has been used in this study.

<sup>\*</sup> Corresponding author: Gamze Fahriye Pehlivan, Department of Architecture, Sivas Cumhuriyet University, Sivas, Turkey, e-mail: geraybat@hotmail.com

2 — Erdener Pehlivan et al. DE GRUYTER

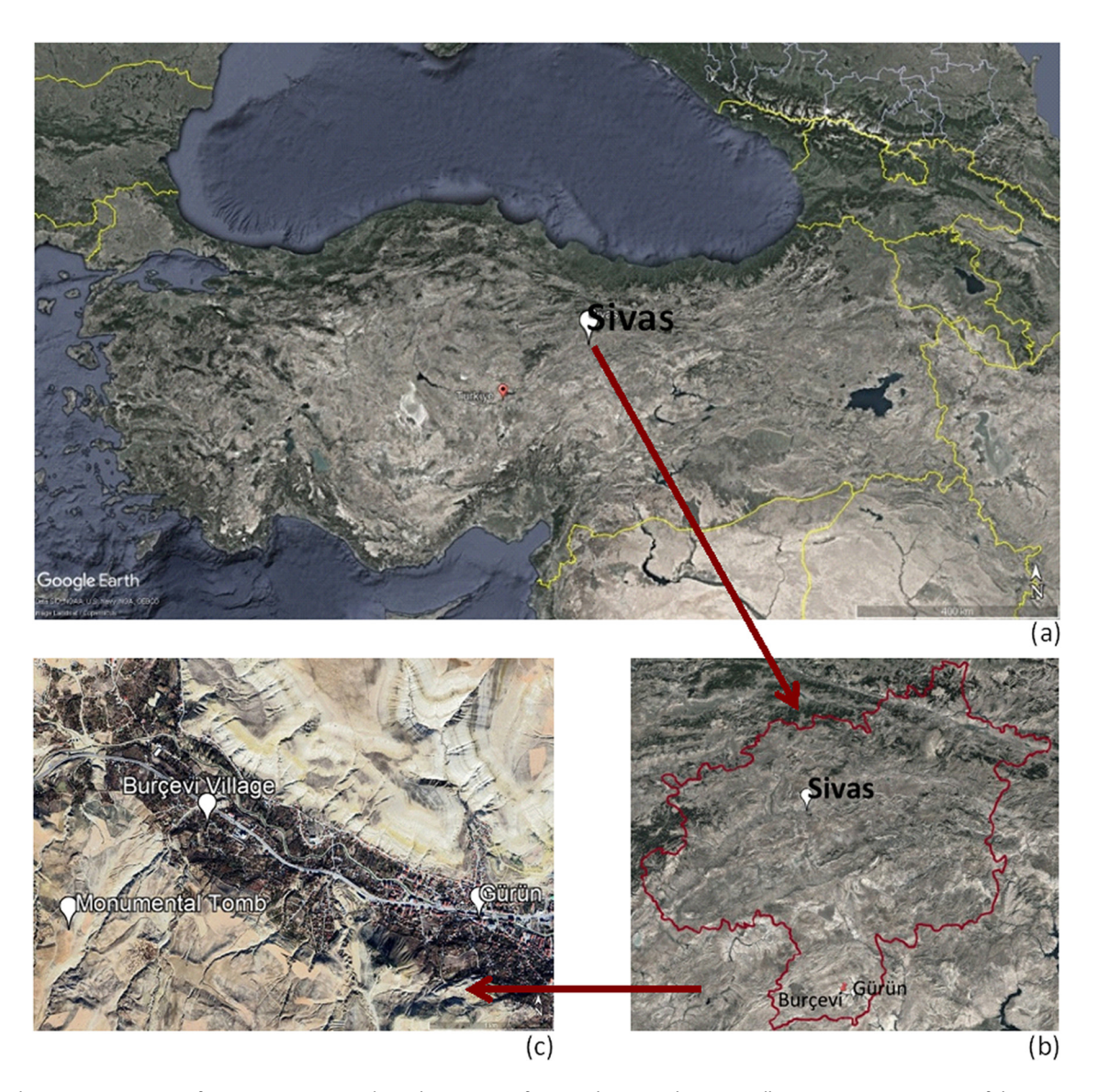


**Figure 1:** (a) Location of Sivas Province in Türkiye. (b) Location of Gürün district and Burçevi Village in Sivas. (c) Location of the Burçevi Monumental Tomb (Google Earth, 2024).

A detailed literature review was conducted on the Burçevi Monumental Tomb, which constitutes the material of this study. The tomb was first noticed and recorded by Von der Osten in 1927–1928 while exploring Gürün, which he described as "a paradise in the middle of the desert." However, it was not extensively detailed² (Von der Osten, 1927–1928, pp. 73–76). The literature review revealed that, aside from the aforementioned publication, the Burçevi Monumental Tomb has not been previously discussed in any scientific article. Therefore, introducing this tomb to the academic literature has become the primary objective of this study. The secondary aim of this study is to utilize analytical methods as a new and contemporary technique to introduce the monumental tomb to the literature and to encourage the adoption of these methods. Additionally, these methods have been employed in the technical research phase aimed at developing conservation strategies for the tomb. The application of these methods in conservation and restoration efforts will help minimize potential issues and errors that may arise during the process.

<sup>2</sup> Additionally, he mentioned the significant natural formations in Gürün, particularly the caves (Von der Osten, 1927–1928, p. 77).

Two different methods were used to define the tomb discussed in this study. First, it was described using the analogical comparison method. In this approach, the tomb was initially documented on-site, and its architecture was examined. Then, similar examples of Roman-period tombs within the Roman world were researched. By comparing similarities in the tomb's roofing, pedestal profiles, niches, façade, and plan features, a dating was proposed. Analogical comparison is a crucial and widely used method for definition in both architectural history and archaeology.

For the analytical definition, X-ray fluorescence (XRF) spectroscopy and Schmidt hammer rebound (SHR) testing were employed. These methods are non-invasive and non-destructive techniques used in the characterization of cultural heritage. They offer a quantitative approach to the definition of cultural heritage. In recent years, scientific studies have started to incorporate the use of XRF and SHR for the analytical identification of cultural heritage (Brookhouse et al., 2020; Columbu et al., 2019; Debailleux, 2018; Ercoli et al., 2012; Eveno et al., 2016; Fugazzotto et al., 2025; Ghigo et al., 2022; Grethe et al., 2020; Haskovic & Ibragic, 2021; Howard et al., 2023; Paz et al., 2024; Tapia et al., 2024; Vanmeert et al., 2022).

Another aim of this study is to promote the use and widespread adoption of these methods in the conservation of cultural heritage in Türkiye.

## 2 Architecture of the Burçevi Monumental Tomb

The tomb, which is the subject of this study, features monumental architecture with a rectangular plan elevated on a krepidoma consisting of three krepis. The structure, which extends in the north-south direction, has its entrance on the northern side (Figure 2). After the level of the krepidoma, six rows of stones have survived to the present day. The kline and the upper cover have not been preserved.

The southern part of the krepidoma has been better preserved as it remained buried under the soil for many years. During the excavation conducted by the Sivas Archaeological Museum in 2018, the southern krepidoma was uncovered. Since part of the lowest krepis is still buried, the height of the riser could not be measured. The width of the first krepis is 33 cm. The riser of the second krepis is 25.5 cm, and its width is 28 cm. The riser of the third krepis is 26 cm, and its width is 30 cm. While the three krepis on the eastern side of the krepidoma are sufficiently preserved, the northern and western sides have been damaged.

The stones used in the wall masonry are rectangular in shape. The north and south walls of the structure are made up of a single row of stones, making them thin, while the east and west walls are thicker, consisting of two rows of stones. The thickness of the walls is as follows: the north wall is 93 cm, the south wall is 80 cm, the east wall is 162 cm, and the west wall is 134 cm. The east and west walls, in fact, were constructed with a thickness of 97 cm up to the second row of stones above the krepidoma level. Starting from the third row, cushion stones were used as consoles to increase the wall width and create a space for the vault (Figure 2).

One of the best-preserved facades of the structure is the northern facade, which also serves as the entrance. There are a total of four plaster elements: two at the corners and two in the middle. The plasters in the center have been particularly damaged. Beneath the corner plasters, there are a base and a plinth with a profile. The plinth is 60 cm wide and 6 cm high. On this facade, two aediculae can be seen starting from the row of stones that forms the door opening, located at the upper right and left corners of the door. The aedicula on the right is immediately to the right of the middle right plaster, with dimensions of 32 cm × 50 cm. The one on the left is immediately to the left of the left plaster, with dimensions of 34 cm × 50 cm. The stone above the door opening is on the verge of falling. This situation can be explained as follows: The lintel stones placed over the opening are usually made in a single piece, and their joints do not align with the door opening. Beneath this stone, the adjacent left stone is broken, and directly opposite, there is no stone on the right, indicating that this stone originally extended across the empty space opposite. In other words, beneath the stone about to fall, there was another monolithic lintel stone (Figure 3). In the western corner of the northern facade, six rows of stones rise, and on the eastern facade, four rows of stones rise. Most of the krepidoma stones on this facade are broken.

4 — Erdener Pehlivan et al. DE GRUYTER

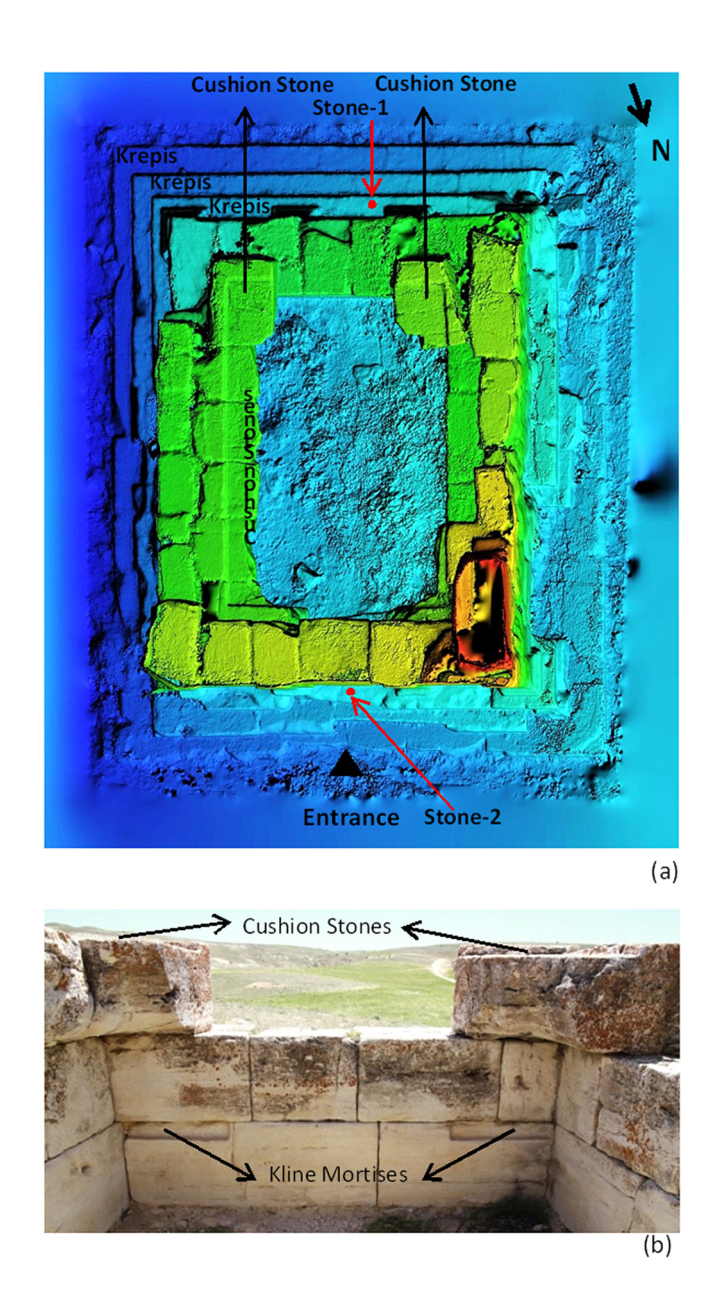


**Figure 2:** (a) DEM analysis of the Burçevi Monumental Tomb. (Red arrows indicate the stones tested. Cushion stones and krepis are marked on the image.) (b) Cushion stones and kline mortises are indicated on the digital photograph.

The southern wall is one of the most heavily damaged sections of the structure. Two rows of stones from the krepidoma are completely preserved, and a few stones from the third row remain in place. There are four plasters on the southern facade. Below these plasters, there is a plinth measuring 60 cm in width, 13 cm in depth, and 6 cm in height. Above the plinth, the base profiles of the plasters are visible. The plasters above these profiles are 39 cm wide and extend 4 cm forward from the wall of the structure (Figure 3).

The eastern facade has been preserved up to the second row of stones at the southern corner, the fourth row of stones at the northern corner, and the third row of stones in the middle (Figure 4). At the level of the third row of stones on this facade, there is a row of cushion stones where the voussoir of the vault, which forms the upper cover of the structure, would have rested. The row of cushion stones provides insight into the structure's roofing (Figure 2). The eastern facade also features a total of four plasters: two at the corners and two in the middle. However, the plasters in the middle have been worn away. Additionally, it has been determined that one of the stones forming the uppermost krepis of the krepidoma on this facade is





**Figure 3:** (a) North Facade of the Monumental Tomb. (The broken lintel stone is partially visible at the location marked by the dashed red line. The other piece of the lintel stone is missing. The stone indicated by the red arrow is the one subjected to testing.) (b) South Facade of the Monumental Tomb (The stone indicated by the red arrow is the one subjected to testing).

missing. While the other stones that form the krepis of the krepidoma remain in place, most are broken (Figure 4).

When the western facade is examined, plasters are found at the southern and northern corners. However, due to significant damage to the wall surface, the plasters that would be expected in the middle section of the wall, as seen on the eastern wall, have not survived due to stone deterioration. The western facade has been preserved up to the third row of stones at the southern corner and up to the sixth row at the northern corner. In the southwestern corner of the western wall, a cushion stone is present. On this facade, some stones of the second krepis have been lost, and those that remain are broken. One stone from the first krepis is missing. Additionally, all stone surfaces exhibit signs of weathering, cracking, and exfoliation (Figure 4).

The excavation of the hyposorion section inside the monument has not been completed. On the southern inner wall, at the upper part of the first row of stones, mortises have been created on both the right and left sides to secure the kline (Figure 2).

# 3 Defining the Burçevi Monumental Tomb through Analogical Comparison

The monumental tomb was analogically compared with other necropolis examples within the Cappadocia Region, neighboring regions, and other tombs located throughout the Anatolian geography. The tradition of monumental tombs, which began with the Nereid Monument in the fourth century BCE, continued to be used increasingly during the Roman Period (Cormack, 2004, p. 21; Özbek, 2007, p. 267). One of the reasons for this is that such tombs were not only commissioned by those who held political power in the city but also by wealthy individuals with sufficient economic means (Gabelmann, 1979, pp. 8–10). Moreover, these types of tombs emphasized the elite status of the deceased while simultaneously aiming to convey this prestige to future generations (Fedak, 1990, pp. 160–161). Although the Cilicia region is considered the origin point of monumental tombs (Cormack, 2004, p. 212; Machatschek, 1967, p. 92), no two monumental tombs are identical in any region (Fedak, 1990, p. 3).

Just above the krepidoma section of the structure, the plaster bases on the plinth have been compared typologically. The first example that shows a similar profile is the lower profile of the pedestal of a statue found *in situ* during the 1970 excavations of the Kaunos Harbor Agora, which is dated to the reign of Emperor Antonius Pius (138–161 CE) and is associated with the son of Sikelia (Çörtük, 2012, pp. 386–387; Marek, 2006, pp. 257–258). Another structure found in the same area is the exedra of Quintius Vedius Capito (Çörtük, 2012,

6 — Erdener Pehlivan et al. DE GRUYTER





Figure 4: (a) East Facade of the Monumental Tomb. (b) West Facade of the Monumental Tomb.

pp. 371–374). This structure, built during the Hadrianic Period in the first half of the second century CE, shares similar features with the Burçevi plaster base.

When examining the tombs in the Cappadocia Region as part of the comparison with the Burçevi Monumental Tomb, the Felahiye Monumental Tomb is one of the examples found in the region. The tomb structure was first identified by Gregoire (Gregoire, 1909, pp. 46–51). Both the Felahiye and Burçevi Monumental Tombs share similarities in their vaulted roofing style. However, the pronaos section found in the Felahiye Monumental Tomb, which is absent in the Burçevi Monumental Tomb, serves as a distinguishing feature between the two structures. The Felahiye Monumental Tomb, with its architectural features,

stylistically reflects characteristics of the second century CE. It is suggested that the plague epidemic that emerged in Mesopotamia during the second century CE (166–189 CE) spread to Anatolia with soldiers from the region, leading to an increase in both death rates and the number of tombs constructed during this period. It is believed that the Felahiye Monumental Tomb was constructed during this time (Cormack, 2004, p. 277; Öztaner, 2012, pp. 369–380).

Another monumental tomb structure identified in Kayseri is located in the Esenyurt neighborhood, in the Tontar area. Brief archaeological work was conducted at the tomb by Kodan and Günbattı. During this work, a coin belonging to Severus Alexander (222–235 CE) was found, leading to the suggestion that the monument may date back to this period (Kodan & Günabattı 1992, pp. 87-88). The tomb has a vaulted roof similar to that of the Burçevi monumental tomb, which is an important feature for establishing regional parallels.

Another monumental tomb in the region is the Ozan Village Monumental Tomb, located in Malatya. The structure is situated 22 km from the Darende district center of Malatya, in Ozan village. The area where the tomb is located was part of the boundaries of the ancient region of Cappadocia. The tomb structure has a square plan with dimensions of 6.65 m × 6.65 m and features a vaulted roof. Two key aspects were considered for the dating of the structure: the use of opus caementicium and the presence of garlands as decorative elements. Based on analogies with similar examples, the structure is dated to the late second century CE-early third century CE (Kaplan et al., 2021, pp. 295-298). The Ozan Village monument also shares similar characteristics with the Burcevi monumental tomb in terms of roof typology.

Another example exhibiting similarities in roof typology with the Burçevi monumental tomb is the tomb designated as T10, located in the city of Elaiussa Sebaste in the Cilicia region. The tomb is dated to the years 150-160 CE. In the study conducted by Durukan, a general chronology and typology of the tombs in the mountainous Cilicia Region were established. One of the key aspects that stood out in this typology was the roof shape and construction technique. Durukan's typology emphasizes three main types, with Type 1 further divided into two subtypes: Type 1a and Type 1b. In Type 1a, the opus caementicium technique is observed, while Type 1b lacks this application (Durukan, 2009, pp. 356–357).

Among the tombs with Type 1b roofs are Elaiussa T10 (150-160 CE), Kanytellis T12 (161-170 CE), Cambazlı 1 (170-180 CE), Cambazlı 2 (161-170 CE), Cambazlı 3 (161-180 CE), Demircili 5 (161-180 CE), and Mezgitkale (170–180 CE) (Durukan, 2009, p. 369). The presence of Cushion stones in the Burçevi tomb suggests that the roof terminates in a vaulted form, and the lack of any traces related to the opus caementicium technique strengthens the possibility that its roof type corresponds to Type 1b, as indicated in Durukan's classification. Another tomb from the Cilicia Region, the Karaböcülü tomb, also exhibits similar characteristics to the Burçevi tomb in terms of roof typology. It is dated to the second and third century CE (Cormack, 2004, pp. 328–329).

From Isauria, the so-called Prostyle Temple Tomb shows similarity to the Burçevi Monumental Tomb only in terms of its roof structure. In terms of decorative elements, the structure displays characteristics of the second century CE (Cormack, 2004, pp. 232–233).

Another tomb located in Lydae in Pamphylia, dated to the late second or early third century CE, also resembles the Burçevi Monumental Tomb in terms of roof typology; however, it differs in having a podium (Cormack, 2004, pp. 238-239).

A tomb from Patara in the Lycian Region also shows similarity with the Burçevi Monumental Tomb due to its vaulted structure. However, it differs in its podium feature and its placement within the terrain (Cormack, 2004, pp. 260-261).

When the structure is evaluated in terms of its niches, the niche found in tomb T10 in the city of Elaiussa Sebaste, mentioned above, resembles the one in the Burçevi Monumental Tomb. Another tomb from the same region is the one located in the Narlıkuyu Solakköy area (Durukan, 2009, pp. 356–357; Söğüt, 2003, p. 245). Another tomb featuring niches in its façade design is the Yelbeyi tomb, located in Yelbeyi neighborhood, Hadim district, Konya province, in the Isauria region (Yılmaz, 2005, pp. 264–266). In the Anemurium necropolis, there are also tombs with niches that resemble those in the Burcevi monument. The niches in Anemurium include decorative elements such as peacock motifs, wreaths, and vine leaves. These tombs are dated to the second and third centuries CE (Alföldi-Rosenbaum, 1971, pp. 35–36; 47; 59; 69). Similar niches have also been identified in some tombs in Roman cities, with these tombs dating to the first and second centuries CE (Hesberg, 1992, p. 88). It is suggested that such tombs began to appear around the second century CE (Durukan, 2012, p. 77).

## 4 Analytical Definition of the Burçevi Monumental Tomb

The analytical technique used to characterize the monumental tomb is XRF spectroscopy. This method is based on the principle that when X-rays irradiate a material, electrons are displaced, and the energy released as electrons from the L shell fill vacancies in the K shell is unique to each element. This characteristic energy can be used to identify the material (Çetinkaya, 2010).

XRF devices can be either desktop or portable. Desktop XRF devices require sampling, which can cause damage to cultural heritage objects, and therefore, are not preferred. In this study, a portable XRF (p-XRF) device was used to obtain non-contact and non-destructive data.

A Thermo Scientific Niton XL3t analyzer with a GOLDD + detector was employed, featuring 60,000 counts per second (cps),  $4\,\mu s$  shaping time, and a spatial resolution of 5 mm, capable of measuring elements from Mg to U. The X-ray tube has a silver anode operating at 50 kV and 200  $\mu A$ . The device also includes an automatic calibration feature.

Measurements were taken for 120 s, holding the device at a distance of approximately 1 mm from the surface at a 90° angle. Three spectral ranges were recorded: 60 – light range, 90 – low range, and 120 – main range.

The measurement data were processed using the manufacturer's software, Standard Thermo Scientific<sup>TM</sup> Niton Data Transfer (NDT<sup>TM</sup>) PC software. This software expresses elemental concentrations as counts per second (cps). Subsequently, the data were converted to parts per million (ppm) and presented graphically.

The SHR test is a method used to determine the hardness and mechanical strength of rocks. This portable device, consisting of a hammer, piston, spring, and outer casing, is held perpendicular to the material surface. The spring-loaded mass is released, and the rebound value created by the energy accumulated in the spring is measured. This value is then converted into an estimated compressive strength using a formula (Kazemi et al., 2019). Based on the obtained data, the strength and hardness classifications of the rocks are determined from the literature.

In this study, a factory-calibrated N-type Schmidt hammer was used. The Schmidt hammer model is JI-355, manufactured by JE  $\dot{I}$ L Precision Industrial Instrument. Ten impacts were applied at a distance of 50 mm from the edge of the stone, at a 90° angle to the surface, and the rebound R values were recorded.

These techniques are non-destructive methods used in the characterization of cultural heritage. These methods, which apply a physical principle without causing damage, can be defined as non-invasive, harmless techniques that do not compromise the visual integrity of the structure and allow analysis to be performed without the need for sample extraction (Bertovic, 2015; Boccacci et al., 2024; Debailleux, 2018; Fredriksen et al., 2020; Fugazzotto et al., 2025; Janssens et al., 2016; Paz et al., 2024; Pehlivan, 2022a; Pehlivan, 2022b; Sharifi & Omrani, 2022; Vanmeert et al., 2022). Recent studies show that non-destructive methods are supported by conservation experts (Shrestha et al., 2022).

The stones of the southern krepidoma, having been buried underground for years, still maintain their original geometry in the shape of regular rectangular prisms. These stones also appear different in color and texture compared to other krepidoma stones. XRF analysis and SHR tests were performed on these distinct surfaces. Stone 1 refers to the upper surface of the stone located in the center of the third krepis on the southern side, which was recently uncovered after being buried underground for years. Stone 2 refers to the upper surface of the stone in the center of the third krepis on the northern side, which has been exposed to atmospheric conditions for many years (Figures 2 and 3). Within the scope of this study, due to time and labor constraints, non-destructive testing methods were applied to only two stones. The reason for testing these two visually different stones was to determine whether they are actually different types of stones.

#### 5 Results

#### 5.1 XRF Spectroscopy

When creating the elemental concentration graph, elements that could not be detected by the XRF device were excluded from the graph, and oxidized forms of elements were removed. Since the results have very small

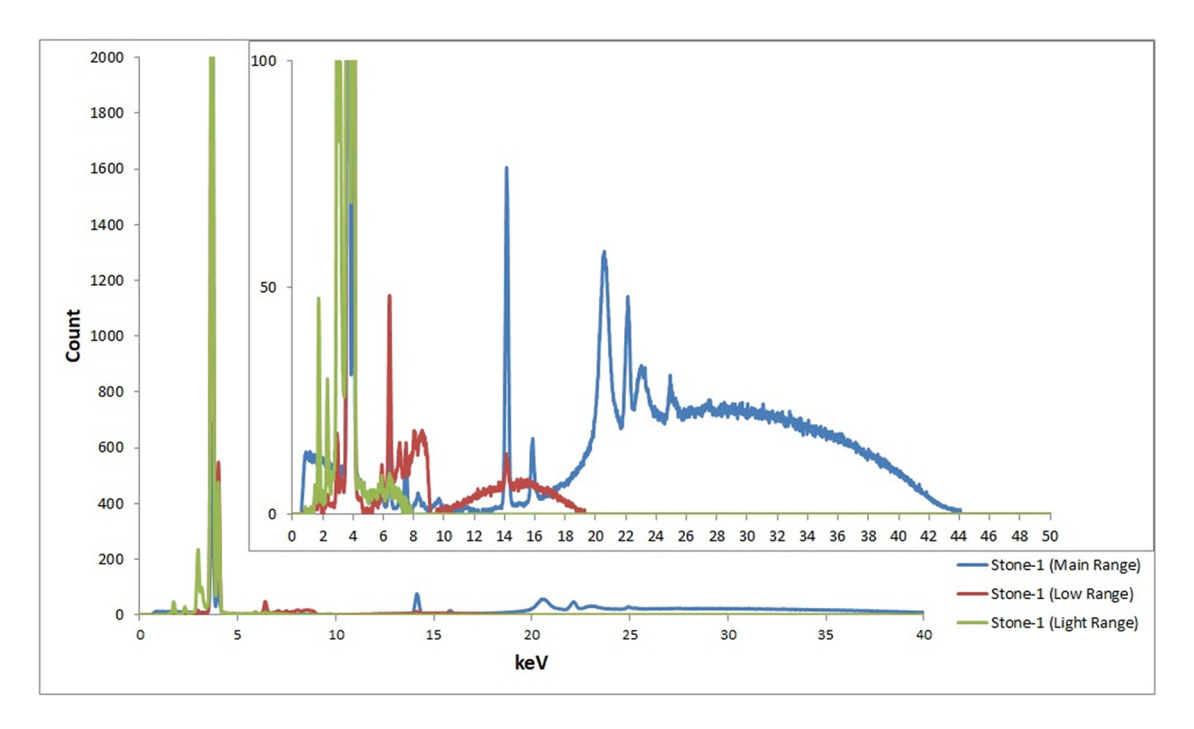


Figure 5: XRF spectrum of Stone 1.

values, they are shown logarithmically in ppm units (Figures 5–8). When the XRF spectra and elemental concentration graphs are evaluated, it is observed that although both stones contain a high concentration of Ca, the Mg content is below 0.2%. Based on this, it is concluded that the examined stones cannot be dolomite but are instead limestone. Elements such as Mn and Fe are found to be at levels too low (below 0.08%) to cause coloration in the stone, while the Si content is determined to be around 7–8%. The high silicon content indicates that the stone is a silicate. Silicification has a strengthening effect on the stone's durability.

When the trace elements in limestone are examined, the presence of Sr is noted. Türkiye is rich in Sr deposits, with 90% of them (as celestine) located in Sivas (Ayaz, 2013, p. 85; Cander et al., 2007, p. 17). Some of these deposits are found in Ulaş, Budaklı, Demirci, Akçamescit, Tahtakeme, Karayün, Akkaya, Battalhöyüğü,

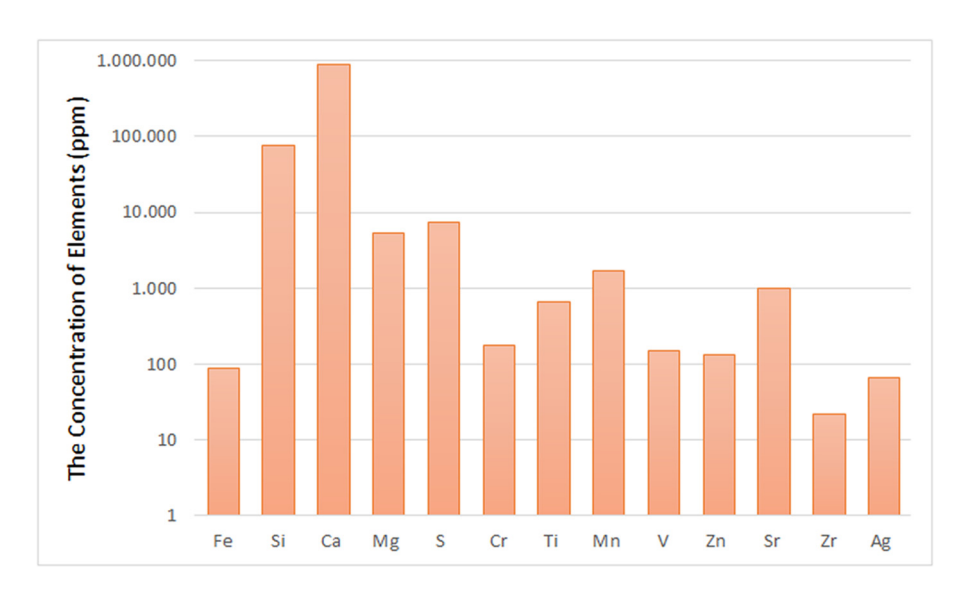


Figure 6: Logarithmic graph of the element concentration in Stone 1.

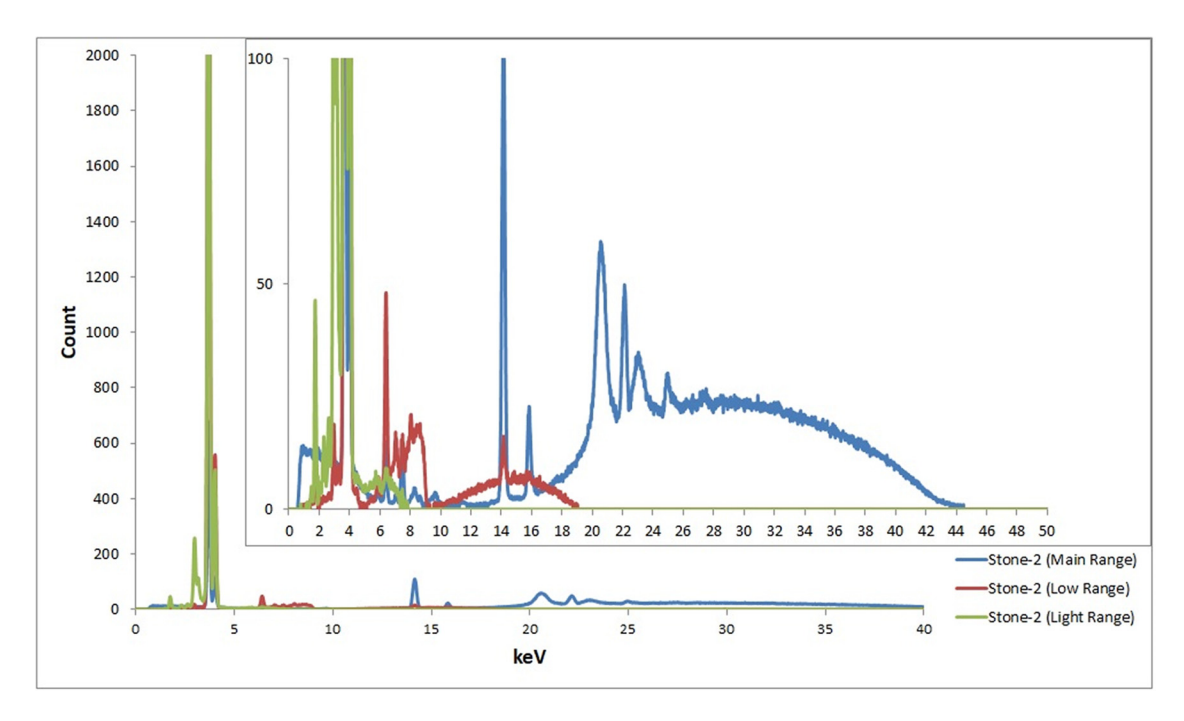


Figure 7: XRF spectrum of Stone 2.

Aşağıada Köyü, Ekincioğlu Köyü, Ayli Köyü, Tilki Tepe, Kadak Köyü, Cerit Köyü, Kabalı Köyü, Tavşanlı Köyü, Ahmetuşağı, Tuzlagözüçatalkaya, Yuva, Alişan Ağılı, Atkıran, Ekinli, Nasır, Sandal, Dipsizgöl, and Kırıkkilise (Demir Şahin et al., 2019, p. 216; Koçan, 2018, pp. 15–17; MTA, 2025; MTA, 2010, p. 6; Ozansoy et al., 1993), as well as in Karalı Köyü (Aktürk & Kayhan, 1988, p. 24), Kavlak, Sinekli, Körtuzla, and Haramçamziyareti (Kıral, 1991, p. 19), and Karagömlek, Pirhüseyin, Ebugen (Ayaz, 2013, p. 75) and Gürün (Palmera et al., 2004, p. 342). Additionally, Sr deposits are present in Hekimhan and Darende, located in the northwestern part of the Malatya bordering Sivas (Palmera et al., 2004, p. 342), as well as in Kuluncak-Başören (MTA, 2020, p. 89).

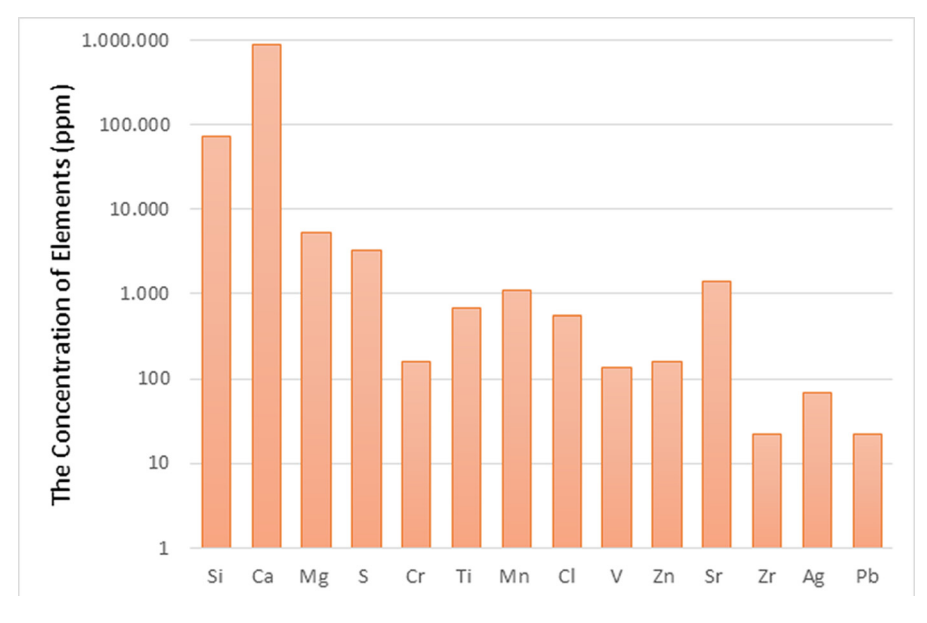
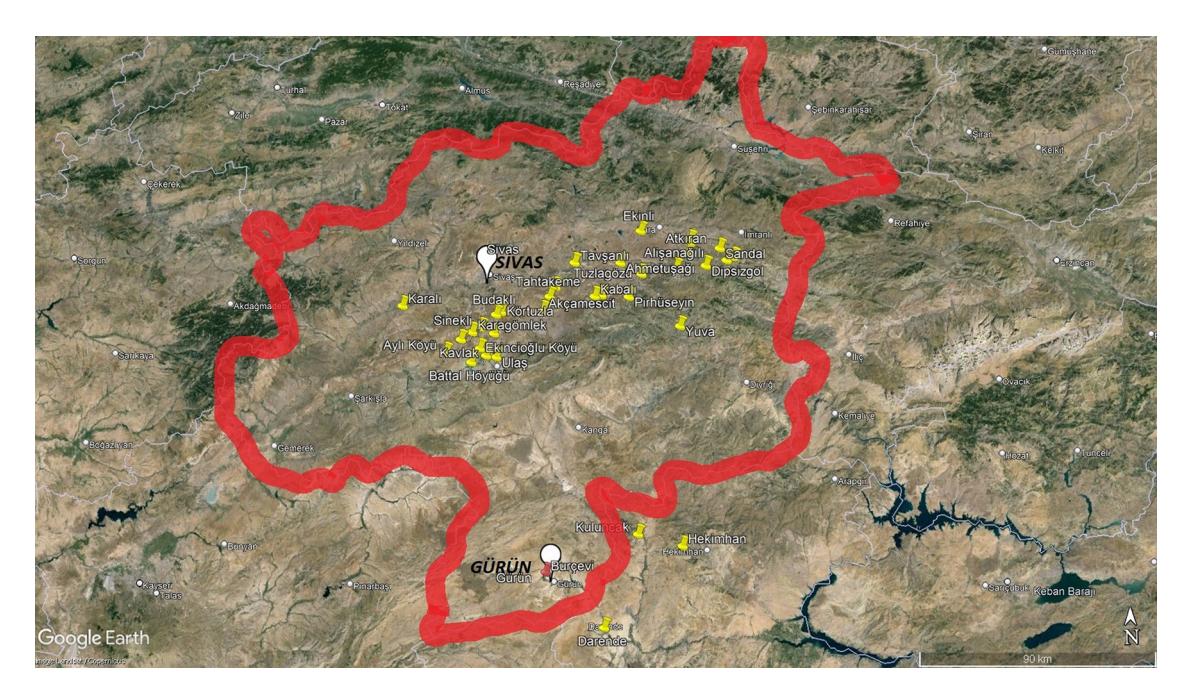


Figure 8: Logarithmic graph of the element concentration in Stone 2.



**Figure 9:** Map showing the Sr deposits around Sivas (Locations marked with yellow dots indicate Sr deposits, while white dots represent the city center of Sivas and the localization of Gürün, where the monumental tomb is situated.) (Google Earth, 2024).

The locations where strontium has been identified around Sivas and the site of the monumental tomb are marked on the map (Figure 9). Accordingly, although strontium deposits are concentrated in the central part of Sivas, strontium is also present in Gürün, where the monumental tomb is located, as well as in Kuluncak, Hekimhan, and Darende, just east of Gürün.

As understood from the MTA map, the location of the Burçevi Monumental Tomb corresponds to the Gürün limestone formation (Figure 10) (Atabey, 1993, p. 99; MTA, 2025; Önal et al., 2004, p. 119). Önal et al. (2004) conducted research on the Gürün limestone formation, collecting samples from the area and compiling a table of their trace elements and oxide compounds. Considering that the Sr element found in the limestone of the monumental tomb is classified as a trace element, the limestone analyses of the tomb were compared with



**Figure 10:** Overlay image of the geological map and actual satellite view of the area where the Burçevi Monumental Tomb is located (The location of the monumental tomb is marked with a black dot. The area shown in gray represents the valley formed by the Tohma River and consists of undifferentiated quaternary deposits. The area shown in yellow [where the tomb is located] is a hill rising from the valley and consists of lacustrine limestone.) (MTA, 2025).

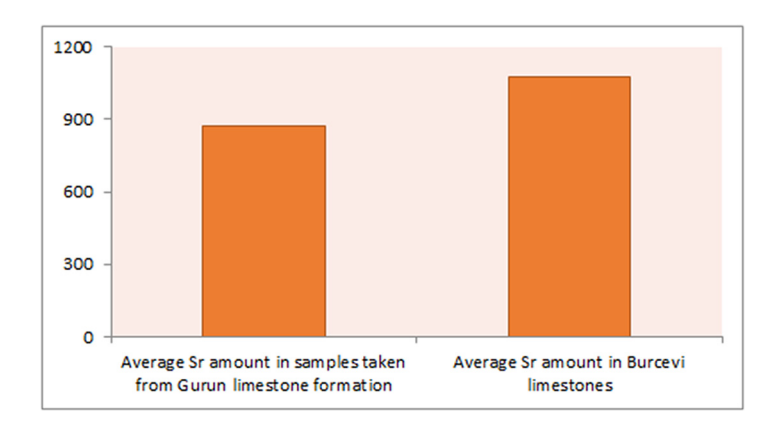


Figure 11: Comparison of Sr Content in Gürün Formation Limestone and Burçevi Limestone (ppm) (Önal et al., 2004, p. 119).

those of the Gürün formation (Önal et al., 2004, p. 119). When these ratios are examined, the Sr content of the stones forming the tomb corresponds with the Sr content of the Gürün limestone formation (Figure 11). This serves as strong evidence that the monumental tomb was likely built using local limestone from this region.

#### 5.2 SHR Tests

In the evaluation of data obtained from the SHR test, extremely high and extremely low values are generally considered suspect. These outlier values are excluded from the assessment. The average of the remaining values is then calculated, and this average value is accepted as the SHR value (ASTM, 2019; ISRM, 2007; Matthews et al., 2014; Sumner & Nel, 2002; USBR, 1998).

As the evaluation method, the internationally recognized ASTM standard was used as the basis. Ten impacts were applied to each stone surface, and the average was then calculated. Values that were seven units above or below the average were considered outliers and excluded, after which a new average was calculated (ASTM, 2019). This new average was accepted as the SHR value and is presented in Table 1.

Many formulas are used to convert the SHR value into an estimated UCS value. The values obtained from these formulas and those from the conversion table on the device are indicated in the table below, and the averages of these values have been calculated (Table 1).

As in the ASTM SHR evaluation method, values that are 7 units above and below the average were excluded from the evaluation, and a new average was calculated. The estimated UCS value is provided in Table 2.

The strength and hardness classifications of the examined stones were determined and tabulated (Table 2). Despite varying classifications in different sources, it can generally be stated that Stone 1 is classified as strong/moderately strong, while Stone 2 is classified as weak. In terms of hardness classification, Stone 1 is categorized as fairly hard rock, and Stone 2 as moderately soft rock.

Tahla	1.	Estimated	IICS	values	(MPa)	according	tο	SHR value
Iable	т.	Estilliateu	0	values	uvirai	accordina	ιυ	onk value

Stones	Average	Conversion of SHR value to estimated UCS (MPa)							
	SHR value	Device conver- sion table	Calculation according to Katz et al. (2000)	Calculation according to Kahraman (2001)	Calculation according to Fener et al. (2005)	Calculation according to Kılıç and Teymen (2008)	Calculation according to Yagiz (2009)	AVR	
Stone 1 Stone 2	46.8 29.4	45.6 18.6	58.5 17.3	40.9 21.2	67.1 24.0	85.4 29.7	58.0 17.4	59.2 21.4	

Table 2: Rock strength classifications and rock hardness classes based on estimated UCS value

Stones	Estimated UCS value (MPa)	The average of SHR value	Rock strength class according to Deere and Miller (1966)*	Rock strength class according to Selby (1980)**	Rock strength class according to ISRM (1981)*	Rock strength class according to Waltham (2009)*	Rock hardness classification according to China (1995) and Wang et al. (2017)*
Stone 1	51.05	46.8	Strong (34–172)	Moderately strong (40–50)	Strong (50-100)	Strong (50–100)	Fairly hard (30–60)
Stone 2	22.1	29.4	Weak (less than 34)	Very weak (10–35)	Weak (5–25)	Moderately strong (12.5–50)	Moderately soft (15–30)

<sup>\*</sup>Classification based on UCS value in the relevant literature.

Table 3: Comparison of estimated UCS values with other limestone UCS values in the literature

UCS values of limestone in the literature (MPa)		Estimated UCS value of limestones 1: 51.05 MPa	Estimated UCS value of limestones 2 22.1 MPa	
According to Teymen (2020)	40.9–140.9	Suitable	Below threshold	
According to Erözmen et al. (2020)	19–24	Suitable	Suitable	
According to Kumral et al. (2019)	Avg 8.3	Suitable	Suitable	
According to Şahin Güçhan et al. (2019)	43.55-81.06	Suitable	Below threshold	
According to Ünal and Beyaz (2019)	7.40–16.20	Suitable	Suitable	
According to Şahin (2018)	14.76-75.07	Suitable	Suitable	
According to Koç et al. (2014)	Avg 13.97	Suitable	Suitable	
According to Karaman and Kesimal (2012)	7.7–18.9	Suitable	Suitable	
According to Dipova (2012)	12.14-116.20	Suitable	Suitable	
According to Tüysüz (2012)	15.4-66.1	Suitable	Suitable	
According to Çobanoğlu et al. (2011)	Avg 71.25	Below average	Below average	
According to Karaman et al. (2011)	8.19–18.85	Suitable	Suitable	
According to Ocak (2008)	Avg 41.01	Suitable	Below average	

A literature review was conducted on limestone extracted from quarries in Türkiye to determine their UCS values. The UCS values of the limestones examined in this study were compared to those obtained for other limestones in Türkiye. If the UCS value was equal to or higher than the values found for other limestones, it was labeled as "suitable." If the value was below this, it was described as "below the threshold or average." Accordingly, it can be said that Stone 1 and Stone 2 have UCS values similar to those of other limestones in Türkiye, and the value is adequate, meaning there are no significant concerns regarding compressive strength (Table 3).

#### 6 Discussion and Conclusion

The Romans, due to the provision in the Leges Duodecim Tabularum, "Hominem mortuum in urbe ne sepelito, neve urito," abandoned the habit of burying their dead inside their homes or within the city. This naturally led to the practice of burial outside the city (Özbek, 2006, pp. 560). This practice explains the absence of any urban elements around the Burçevi Monumental Tomb.

<sup>\*\*</sup>Classification based on SHR value in the relevant literature.

During the reign of Archelaus, the last king of Cappadocia (36 BC–17 AD), the hegemony of the Roman Empire in the region was clearly felt. However, following this period, when the region became a province of the Roman Empire, the types of tombs also reflected this change. During this period, while the number of tumulus tombs decreased, the number of monumental tombs increased. These necropolis elements are significant evidence of the acceleration of the Romanization process in the region and in Anatolia. Monumental tombs, which began to be seen during the reign of Hadrian (Morris, 1992), became widespread during the reign of Septimius Severus. Based on this information, Durukan dates these types of tombs to the mid-second century AD (Durukan, 2012, pp. 60). Additionally, there may be a correlation between the rise in the number of tombs and the plague epidemic that emerged in Mesopotamia in the second century AD. It is also possible to think that the Legio XII Fulminata, which controlled the eastern border of Cappadocia during this period, was affected by this situation. As Baz mentions, it is likely that soldiers who retired from this legion, stationed in Melitene, returned to their hometowns and were buried in local monumental tombs, such as the one at Ozan village (Takmer & Baz, 2017, pp. 176–187).

In the analogical comparison of the monumental tomb, data supporting the above dating have been obtained. When evaluating the pedestal profiles on the krepidoma, it is observed that this type of profile was used throughout the second century AD. From an architectural perspective, the tomb structure, compared typologically with examples in both the immediate vicinity and neighboring regions, can be dated to the second half of the second century AD. The increased number of tombs due to the plague epidemic in the historical context, the typology of tombs brought by the Romanization process to Anatolia, and the architectural features of these tombs support this dating. The fact that this structure is the only known example within the borders of Sivas province in the second century AD is of great significance in terms of reflecting the Roman Imperial Period burial traditions in the Anatolian geography. The analogical approach discussed in this article is crucial for ensuring the monumental tomb's place in the archaeological world.

The construction of the monumental tomb is not merely a burial ritual; it should undoubtedly be regarded as one of the most tangible ways to emphasize the Roman identity and elite status of a Roman elite (soldier). Accordingly, a monumental tomb allows us to interpret a person's social status and economic power.

As a result of the analytical approach, it was determined that the stones, which appeared different from each other, are actually identical; the tomb monument is made of limestone, and its trace element composition corresponds to that of the Gürün Formation. In other words, it can be said that local limestone was used in the Burçevi Monumental Tomb.

Although Rome had the means to bring stones from other locations outside the local quarry – as examples of monumental architecture show – the use of local labor and material in the context of necropolis elements is more rational, in accordance with Roman pragmatism. Therefore, it is evident that local material was used.

According to the SHR tests, it is observed that the compressive strengths of the limestones from the quarries currently in use in Türkiye are generally close to those of the stones used in the monument. However, another notable result from the SHR test is that, despite two stones being of the same type according to XRF analysis, they have different SHR test results. Stone 1 is classified as strong/moderately strong and fairly hard rock, while Stone 2 is classified as weak and moderately soft rock. The reason for this discrepancy is that Stone 2 has been exposed to long-term atmospheric conditions. In other words, repeated atmospheric events such as water absorption, evaporation, freezing, and thawing over many years have caused degradation in the material, resulting in a loss of strength. On the other hand, Stone 1, which has been buried underground for many years and recently uncovered through archaeological excavation, has not been exposed to these effects. Thus, it has benefited from the natural protective conditions of being buried in the soil. This has helped preserve its strength.

The results bring up a topic that has been debated for years: Can archaeological excavations, which are one of the most fundamental methods of resolving questions in science, also be seen as an action that initiates the process of deterioration? In fact, this awareness emphasizes the need for archaeological excavations to be conducted not in a way that halts them altogether, but rather in a controlled and careful manner where necessary.

Acknowledgments: We would like to thank the Metallurgical and Materials Engineer Assoc. Prof. Dr. Ali ÖZER for his support in this study.

Funding information: The authors state that no funding is involved.

Author contributions: All authors agree to submit the manuscript to this journal, take responsibility for the content, have reviewed all results, and approved the final version of the manuscript. Fieldwork, on-site observations, study design, and conceptualization were conducted by E.P., A.A., and G.F.P.; architectural studies of the tomb were carried out by E.P. and G.F.P. E.P. carried out archaeological research using analogical comparison methods, while G.F.P. conducted the analytical investigations. Visuals and tables were prepared by E.P. and G.F.P. G.F.P. prepared the manuscript with contributions from all co-authors.

Conflict of interest: The authors state no conflict of interest.

Data availability statement: The data sets generated and analyzed during the current study are available from the corresponding author on reasonable request.

#### References

Aktürk, A., & Kayhan, T. (1988). Sivas (Hafik – Karalık Köyü) Stronsiyum Yatağının Jeolojisi ve Oluşumu. Jeoloji Kurultayı TMMOB jeoloji Mühendisleri Odası, 42, 24-25.

Alföldi-Rosenbaum, E. (1971). Anamur Nekropolisi. Türk Tarih Kurumu Basımevi.

ASTM. (2019). Standard test method for determination of rock hardness by rebound hammer method. ASTM Stand. D 5873-05.

Atabey, E. (1993). Gürün Otoktonu'nun Stratigrafisi (Gürün - Sarız Arası), Doğu Toroslar - Gb Sivas. Türkiye Jeoloji Bülteni, 36, 99-113.

Ayaz, E. M. (2013), Sivas Yöresinin Karmasık Jeolojik Yapısına Bağlı Olarak Gelisen Önemli Maden Yatakları Ve MTA'nın Sivas Yöresindeki Yeni Bulquları. MTA Ekonomi Bülteni, Sayı.16, 65-87. https://www.mta.gov.tr/v3.0/sayfalar/hizmetler/kutuphane/ekonomibultenleri/ 2013 16/65.pdf.

Bertovic, M. (2015). Human factors in non-destructive testing (NDT): Risks and challenges of mechanised NDT (Order No. 10735735). Available from ProQuest Dissertations & Theses Global. (2082106258). doi: 10.14279/depositonce-4685. Retrieved from https://www. proquest.com/dissertations-theses/human-factors-non-destructive-testing-ndt-risks/docview/2082106258/se-2.

Boccacci, G., Frasca, F., Bertolin, C., & Siani, M. A. (2024). Diagnosis of historic reinforced concrete buildings: A literature review of nondestructive testing (NDT) techniques. Procedia Structural Integrity, 55, 160-167. doi: 10.1016/j.prostr.2024.02.021.

Brookhouse, M., Ives, S., Dredge, P., Howard, D., & Bridge, M. (2020). Mapping Henry: Dendrochronological analysis of a sixteenthcentury panel painting based upon synchrotron-sourced X-ray fluorescence mapping. Studies in Conservation, 66(7), 384-396. doi: 10.1080/00393630.2020.1848133.

Cander, Y., Gerim, İ., & Altunay, A. (2007). Madencilik Özel İhtisas Raporu, Dokuzuncu Kalkınma Planı 2007-2013, T.C. Başbakanlık Devlet Planlama Teşkilatı.

Çetinkaya, T. (2010). Yüzey Modifiye Edilmiş Nanokompozit Killerde XRF Karakterizasyonu. (Yayımlanmamış Yüksek Lisans Tezi). Sakarya Üniversitesi.

China NSotPsRo. (1995). Standard for engineering classification of rock masses (GB50218-94). China Planning Press.

Çobanoğlu, İ., Koralay, T., Kaya, A., & Çelik, S. B. (2011). Investigation the Usability of Limestone Blocks in Karatepe Melange (Kaklık-Denizli) In Production of Concrete Aggregate. 6th International Aggregate Symposium. Sivas, Turkey, October 6-7 (pp. 215-223).

Columbu, S., Gioncada, A., Lezzerini, M., & Sitzia, F. (2019). Mineralogical-chemical alteration and origin of ignimbritic stones used in the old cathedral of Nostra Signora di Castro (Sardinia, Italy). Studies in Conservation, 64(7), 397-422. doi: 10.1080/00393630.2018. 1565016.

Cormack, S. (2004). The space of death in Roman Asia minor. Phoibos Verlag.

Çörtük, U. (2012). Kaunos Liman Agorası Anıtları. Ege Üniversitesi, Sosyal Bilimler Enstitüsü, Arkeoloji Ana Bilim Dalı, Yayımlanmamış Doktora Tezi, İzmir.

Debailleux, L. (2018). Schmidt hammer rebound hardness tests for the characterization of ancient fired clay bricks. International Journal of Architectural Heritage, 13(2), 288-297. doi: 10.1080/15583058.2018.1436204.

Deere, D. U., & Miller, P. R. (1966). Engineeing classification and index proporties for intact rock, Technical Report No. Afwl-Tr-65-116, (pp. 9-300): Air Force Weapons Laboratory Research and Technology Division.

Demir Şahin, Ç., Uçurum, A., & Efe, A. (2019). Akkaya Sölestin Yatağının Jeolojisi, Mineralojik Petrografik Özellikleri Ve İzotop (Sr, S, O, H) Jeokimyası (Ulaş, Sivas-Türkiye). KSÜ Mühendislik Bilimleri Dergisi, 22(4), 215–237.

- Dipova, N. (2012). Investigation of the relationships between abrasiveness and strength properties of weak limestones along a tunnel route. *Jeoloji Mühendisliği Dergisi*, *36*(1), 23–34.
- Durukan, M. (2009). Chronology of the temple tombs in Rough Cilicia. Byzas, 9, 343-370.
- Durukan, M. (2012). Kappadokia'da, Argaios Dağı çevresinde Hellenistik-Roma dönemi mezarları ve ölü kültü: Gräber und Totenkult in der hellenistisch-römischen Zeit in der Umqebung des Argaios in Kapadokien. Arkeoloji ve Sanat Yayınları.
- Ercoli, L., Megna, B., Nocilla, A., & Zimbardo, M. (2012). Measure of a limestone weathering degree using laser scanner. *International Journal of Architectural Heritage*, 7(5), 591–607. doi: 10.1080/15583058.2012.654893.
- Erözmen, T., Ündül, Ö., & Aysal, N. (2020). Evaluation for the effects of different cleaning techniques applied on Küfeki Stones Used in historical buildings in İstanbul. *Pamukkale University Journal of Engineering Sciences*, 26(8), 1413–1418.
- Eveno, M., Mysak, E., Müller, K., Bastian, G., Pincas, N., & Reiche, I. (2016). Confocal XRF depth profiling non-destructively reveals the original blue pigments in a Renaissance painting by Caroto. *Studies in Conservation*, *61*(2), 102–112. doi: 10.1080/00393630.2016. 1142059
- Fedak, J. (1990). Monumental tombs of the Hellenistic Age: A study of selected tombs from the pre-classical to the early imperial era. University of Toronto Press.
- Fener, M., Kahraman, S., Bilgil, A., & Gunaydin, O. (2005). A comparative evaluation of indirect methods to estimate the compressive strength of rocks. *Rock Mechanics and Rock Engineering*, 38(4), 329–343.
- Fredriksen, P. D., Rødsrud, C. L., & Caruso, F. (2020). What happened at augland? a social chronology for the demise of a roman iron age ceramic workshop in south norway. *Oxford Journal of Archaeology*, *39*, 442–464. doi: 10.1111/ojoa.12204.
- Fugazzotto, M., Caggiani, M. C., Spironello, M. Y., Barone, G., & Mazzoleni, P. (2025). First insight into gemstones on historical ecclesiastical artefacts in Sicily (17th–19th centuries): A non-invasive survey. *Archaeometry*, *67*(4), 966–983. doi: 10.1111/arcm.13059.
- Gabelmann, H. (1979). *Römische Grabbauten der frühen Kaiserzeit*. Gesellschaft für Vor- und Frühgeschichte in Württemburg und Hohenzollern e.V. mit Unterstützung des Württembergischen Landesmuseums Stuttgart und der Stadt Aalen.
- Ghigo, T., Bone, D., Howell, D., Domoney, K., Gironda, M., & Beeby, A. (2022). Material characterisation of William Burges' great bookcase within the disruption of a global pandemic. *Studies in Conservation*, *69*(1), 1–16. doi: 10.1080/00393630.2022.2153463.
- Google Earth. (2024). (Last Accessed: 15.09.2024).
- Grégoire, H. (1909). Voyage dans le Pont et en Cappadoce. BCH, 33, s.46-51, lev.7-10.
- Grethe, R., Karydas, A. G., Kantarelou, V., & Zacharias, N. (2020). Micro-XRF analysis of silver decorations on Archaic helmets from Olympia. *Archaeometry*, *62*, 974–990. doi: 10.1111/arcm.12561.
- Haskovic, A., & Ibragic, S. (2021). Use of analytical methods in revealing the techniques of Ottoman calligraphers: An illuminated manuscript from the eighteenth century. *Studies in Conservation*, *67*(5), 313–326. doi: 10.1080/00393630.2021.1885785. Hesberg, H. V. (1992). *Romische Grabbauten*.
- Hild, F., & Restle, M. (1981). Tabula İmperi Byzantini Band 2 Kappadokien. Verlag der Österreichiscen Akademie der Wissenschaften.
- Howard, H., Najorka, J., Schofield, P. F., & Geraki, K. (2023). Degradation of fourteenth-century mordant gilding layers: Synchrotron-based microfocus XRF, XRD, and XANES analyses of two paintings by Pietro Lorenzetti. *Studies in Conservation*, *69*(3), 193–208. doi: 10.1080/00393630.2023.2201094.
- ISRM. (1981). Rock characterization, testing and monitoring. International Society for Rock Mechanics, Suggested Methods.
- ISRM. (2007). The complete ISRM suggested methods for rock characterization, testing and monitoring, (pp. 153–154). R. Ulusay & J. A. Hudson, Eds. Kozan Offset Press.
- Janssens, K., Van der Snickt, G., Vanmeert, F., Legrand, S., Nuyts, G., Alfeld, M., Monico, L., Anaf, W., De Nolf, W., Vermeulen, M., & Verbeeck, J. (2016). Non-invasive and non-destructive examination of artistic pigments, paints, and paintings by means of X-ray methods. *Topics in Current Chemistry (Z), 374*, 81. doi: 10.1007/s41061-016-0079-2.
- Kahraman, S. (2001). Evaluation of simple methods for assessing the uniaxial compressive strength of rock. *International Journal of Rock Mechanics and Mining Sciences*, *38*(7), 981–994.
- Kaplan, D., Koçak, İ. E., & Alkan, A. (2021). Kappadokia'da Bir Anıt: Ozan Köyü Anıt Mezarı ve Legio XII Fulminata. OLBA, XXIX, 287–312. Karaman, K., Erçıkdı, B., Cihangir, F., & Kesimal, A. (2011). Examining the schmidt hammer methods in estimation of the uniaxial compressive strength. Türkiye 22. Uluslararası Madencilik Kongresi ve Sergisi, 11–13 Mayıs 2011, Ankara [online, cited 01.08.2022]. https://www.researchgate.net/publication/267781874.
- Karaman, K., & Kesimal, A. (2012). Kayaçların Tek Eksenli Basınç Dayanımı Tahmininde Nokta Yükü Deney Yöntemleri ve Porozitenin Değerlendirilmesi. *Madencilik*, *51*(4), 3–14.
- Katz, O., Rechesa, Z., & Roegiersc, J. C. (2000). Evaluation of mechanical rock properties using a Schmidt hammer. *International Journal of Rock Mechanics and Mining Sciences*, *37*(4), 723–728.
- Kazemi, M., Madandoust, R., & Brito, J. (2019). Compressive strength assessment of recycled aggregate concrete using Schmidt rebound hammer and core testing. *Construction and Building Materials*, *224*, 630–638, doi: 10.1016/j.conbuildmat.2019.07.110.
- Kılıç, A., & Teymen, A. (2008). Determination of mechanical properties of rocks using simple methods. *Bulletin of Engineering Geology and the Environment*, *67*, 237–244.
- Kıral, N. (1991). Sivas Ulaş Sölestin Yatağının Jeolojisi ve Ekonomik Değerlendirilmesi. Anadolu Üniversitesi, Fen Bilimleri Enstitüsü,
- Κος, E., Demir Şahin, D., & Yılmaz, A. O. (2014). Examination of indirect tensile and point load strength on different originated rock samples taken between Trabzon-Macka areas. ROCKMEC'2014-XI th Regional Rock Mechanics Symposium, Afyonkarahisar, Turkey.
- Koçan, F. (2018). Sivas Bölgesi Selestit Cevherinin Asit Ve Baz Çözeltileri İle Çözünme Kinetiği Ve SrCrO4 Üretimi. Manisa Celal Bayar Üniversitesi Fen Bilimleri Enstitüsü.

- Kodan, H., & Günabattı, C. (1992). Tontar Roma Mezarı. Türk Arkeoloji Dergisi, 50, 83-103.
- Kumral, M., Şans, G., Yalçın, C., Kaya, M., & Budakoğlu, M. (2019). The effects of physical and chemical properties on the formation of historical kufeki stone in Catalca (Istanbul). Omer Halisdemir University Journal of Engineering Sciences, 8(1), 278-287.
- Machatschek, A. (1967). Die Nekropolen und Grabmäler im Gebiet von Elaiussa Sebaste und Korykos im Rauhen Kilikien. Böhlau.
- Marek, C. (2006). Die Inschriften von Kaunos, Vestiga Band 55. Verlag C. H. Beck.
- Matthews, J. A., Winkler, S., & Wilson, P. (2014). Age and origin of ice-cored moraines In Jotunheimen and Breheimen, Southern Norway: Insights from Schmidt-Hammer exposure-age dating. Geografiska Annaler: Series A, Physical Geography, 96, 531-548. doi: 10.1111/ geoa.12046.
- Morris, I. (1992). Death-ritual and social structure in classical antiquity.
- MTA. (2010). MTA Harita. https://www.mta.gov.tr/v3.0/sayfalar/bilgi-merkezi/maden\_potansiyel\_2010/sivas\_madenler.pdf (Last Accessed: 02.07.2023).
- MTA. (2020). MTA Faaliyet Raporu. https://www.mta.gov.tr/v3.0/sayfalar/kurumsal/belgeler/2020-Faaliyet-Raporu.pdf.
- MTA. (2025). Flourit Fosfat Jips Sofratuzu Kükürt Sölestin (Stronsiyum) Yatakları Haritası. https://www.mta.gov.tr/v3.0/sayfalar/hizmetler/ images/b h/f-p-ips-Na-S-Sr.ipg (Last Accessed: 23.01.2025).
- Ocak, İ. (2008). Tek Eksenli Basınc Dayanımını Kullanarak Kaya Malzemesinin Elastisite Modülünün Tahmini. İstanbul Yerbilimleri Dergisi, 21(2), 91-97.
- Önal, M., Helvaci, C., & Ceyhan, F. (2004). Geology and trona potential of the middle Miocene Gurun (Sivas) Basin, Central Anatolia, Turkey. Carbonates and Evaporites, 19(2), 118-132.
- Ozansoy, C., Özsoy, S. S., Kayan, T., & Çubuk, Y. (1993). Battalhöyüğü Tepe (Ulaş-Sivas) Öir:3669, Ar:39575 No'lu Sölestin Ruhsat Sahası Sondajlı Çalışmalar Ve Detay Jeoloji Raporu., Maden Etüt ve Arama Dairesi Başkanlığı.
- Özbek, Ç. (2006). Roma Dönemi'nde Anadolu'da Ölü Gömme Geleneği ve Ölü Kültü. Hayat Erkanal'a Armağan Kültürlerin Yansıması (pp. 560-563). Homer Kitabevi.
- Özbek, Ç. (2007). Anadolu'nun Hellenistik ve Roma Dönemi Anıt Mezar Geleneğine Genel Bir Bakış, Coşkun Özgünel'e 65. Yaş Armağanı (pp. 265-271). Homer Kitabevi.
- Öztaner, S. H. (2012). Kappadokia Bölgesi'nden Tapınak Planlı Bir Anıt Mezar: Kayseri Felahiye Mezar Anıtı. Belleten, 76(276), 369–384. Palmera, M. R., Helvacı, C., & Fallickc, A. E. (2004). Sulphur, sulphate oxygen and strontium isotope composition of Cenozoic Turkish evaporites. Chemical Geology, 209, 341-356.
- Paz, S., Jorge, A. D., José, R., João, C., & Giacomo, D. (2024). Evaluation of the mechanical characteristics of marble using non-destructive techniques: Ultrasound versus Schmidt hammer rebound tests. In B. T. Herrán & D. Bienvenido-Huertas (Eds.), Woodhead publishing series civil and structural engineering, diagnosis of heritage buildings by non-destructive techniques (pp. 551-574). Woodhead Publishing. doi: 10.1016/B978-0-443-16001-1.00021-8.
- Pehlivan, E. (2022a). Archaeological evaluation and provenance analysis of apollon's torso in sivas archaeological museum. Mediterranean Archaeology and Archaeometry, 22(1), 97-109.
- Pehlivan, G. F. (2022b). Kültürel miras yapılarında taş malzemenin tahribatsız XRF yöntemiyle analizi: Şirinoğlu Hamamı örneği. KAPU Trakya Journal of Architecture and Design, 2(2), 57-68.
- Şahin, M. (2018). Nokta Yükü Dayanım İndeksinin Yarılanmış Karot Örneklerinden Belirlenebilirliğinin Araştırılması. Hacettepe Üniversitesi, Jeoloji Mühendisliği Anabilim Dalı.
- Şahin Güçhan, N., Bilecen, K., Warscheid, T., Topal, T., Son, Ç., Çıplak, E. S., Ersöz, T., Kaya, Y., & Öztürk, M. (2019). Tarihi Kireçtaşlarını Koruma Müdahalelerinde Uygulamak Üzere Kalsit Üreten Bakterilerle Biyolojik Harç Gelistirilmesi, Program Kodu: 1001, Proje No: 115M188. TÜBİTAK ARDEB.
- Selby, M. J. (1980). A rock mass strength classification for geomorphic purposes: With test from Antarctica and New Zealand. Zeitschrift für Geomorphologie, 24, 31-51.
- Sharifi, M., & Omrani, B. (2022). A laboratory analysis of the Kura-Araxes pottery from Tepe Pirtaj using petrography and XRF techniques. Archaeometry, 64(4), 883-897. doi: 10.1111/arcm.12751.
- Shrestha, R., Sfarra, S., Ridolfi, S., Gargiulo, G., & Kim, W. (2022). A numerical-thermal-thermographic NDT evaluation of an ancient marquetry integrated with X-ray and XRF surveys. Journal of Thermal Analysis and Calorimetry, 147, 2265-2279.
- Söğüt, B. (2003). Dağlık Kilikia Bölgesi Mezar Nişleri. Olba, VII (Özel Sayı), 239–262.
- Sumner, P., & Nel, W. (2002). The effect of moisture on schmidt hammer rebound: Tests on rock samples from Marion Island and South Africa. Earth Surface Processes and Landforms, 27, 1137–1142.
- Takmer, B., & Baz, F. (2017). The Gravestone of C. Iulius, optio of the Legio XII Fulminata. Philia III, 176-187.
- Tapia, J., Eveno, M., Arias P., Ontañón, R., Schöder, S., Müller, K., & Reiche, I. (2024). Improving the characterization of red coloring matter from prehistoric cave art by means of laboratory confocal XRF depth profiling combined with synchrotron XRF imaging. Journal of Cultural Heritage, 67, 385-394. doi: 10.1016/j.culher.2024.03.018.
- Teymen, A. (2020). Estimation of uniaxial compressive strength of very low-medium abrasive rocks from Cerchar abrasiveness index. Pamukkale Univ Muh Bilim Dergi, 26(6), 1154-1163.
- Tüysüz, L. (2012). İstanbul'da Açılacak Metro Tünellerinde Tbm (Tünel Açma Makinesi) Performansını Tahmin Etmek İçin Yeni Bir Yaklaşım, p. 19, İstanbul Teknik Üniversitesi, Fen Bilimleri Enstitüsü, Maden Mühendisliği Anabilim Dalı, Yüksek Lisans Tezi.
- Ünal, M., & Beyaz, T. (2019). Hasankeyf Kireçtaşlarının Suda Dağılmaya ve Tuz Kristalleşmesine Karşı Direncinin Araştırılması. Engineering Sciences, 14(2), 55-62.
- USBR. (1998). Engineering geology field manual. Field index tests, (Vol. 1, pp. 111-120). US Government Printting Office.

Vanmeert, F., De Meyer, S., Gestels, A., Clerici, E. A., Deleu, N., Legrand, S., Van Espen, P., Van der Snickt, G., Alfeld, M., Dik, J., & Monico, L. (2022). Non-invasive and non-destructive examination of artists' pigments, paints and paintings by means of X-ray imaging methods. In: M. P. Colombini, I. Degano, & A. Nevin (Eds.), Analytical chemistry for the study of paintings and the detection of forgeries. *Cultural heritage science.* Springer. doi: 10.1007/978-3-030-86865-9\_11.

Von Der Osten, H. H. (1927–1928). Explorations in Hittite Asia Minor. The University of Chicago Press.

Waltham, T. (2009). Foundations of engineering geology, (3rd ed., p. 49). Spon Press Taylor & Francis.

Wang, H., Lin, H., & Cao, P. (2017). Correlation of UCS rating with Schmidt hammer surface hardness for rock mass classification. Rock Mechanics and Rock Engineering, 50, 195-203. doi: 10.1007/s00603-016-1044-7.

Yagiz, S. (2009). Predicting uniaxial compressive strength, modulus of elasticity and index properties of rocks using the Schmidt hammer. Bulletin of Engineering Geology and the Environment, 68(1), 55-63.

Yılmaz, M. (2005). Bozkır Çevresinin (Hadim - Ahırlı - Yalıhüyük) Antik Tarihi ve Eserleri. Selçuk Üniversitesi Basımevi.